

Simulation of optically conditioned retention and mass occurrences of *Periphylla periphylla*

NICOLAS DUPONT* AND DAG L. AKSNES

DEPARTMENT OF BIOLOGY, UNIVERSITY OF BERGEN, PO BOX 7803, N-5020 BERGEN, NORWAY

*CORRESPONDING AUTHOR: nicolas.dupont@bio.uib.no

Received August 31, 2009; accepted in principle December 18, 2009; accepted for publication January 22, 2010

Corresponding editor: Mark J. Gibbons

Jellyfish blooms are of increasing concern in many parts of the world, and in Norwegian fjords an apparent increase in mass occurrences of the deep water jellyfish *Periphylla periphylla* has attracted attention. Here we investigate the hypothesis that changes in the water column light attenuation might cause local retention and thereby facilitate mass occurrences. We use a previously tested individual-based model of light-mediated vertical migration in *P. periphylla* to simulate how retention is affected by changes in light attenuation. Our results suggest that light attenuation, in combination with advection, has a two-sided effect on retention and that three fjord categories can be defined. In category 1, increased light attenuation turns fjords into dark “deep-sea” environments which increase the habitat and retention of *P. periphylla*. In category 2, an optimal light attenuation facilitates the maximum retention and likelihood for mass occurrences. In category 3, further increase in light attenuation, however, shoals the habitat so that individuals are increasingly exposed to advection and this results in loss of individuals and decreased retention. This classification requires accurate determinations of the organism’s light preference, the water column light attenuation and topographical characteristics affecting advection.

KEYWORDS: *Periphylla periphylla*; diel vertical migration; light attenuation; advection; optical retention

INTRODUCTION

Blooms of jellyfishes (Mills, 2001) have been reported from every part of the world during the last century (Purcell *et al.*, 2007). Such blooms are of increasing concern because of negative impacts on human activities such as fisheries, mariculture, electricity production and tourism (Mills, 2001; Purcell and Arai, 2001). Potential causes have been investigated in different places of the world, and factors such as temperature (Purcell *et al.*, 1999; Purcell, 2005), salinity (Purcell *et al.*, 1999; Purcell, 2005), pH (Attrill *et al.*, 2007), North

Atlantic Oscillation (NAO) (Lynam *et al.*, 2004; Purcell, 2005; Attrill *et al.*, 2007) and the light regime (Sørnes *et al.*, 2007; Lo *et al.*, 2008) have been addressed.

Periphylla periphylla (Péron and Lesueur 1820) is a coronate scyphomedusa of the family Periphyllidae and is considered to be a deep water species with a global distribution. The most studied mass occurrence of *P. periphylla* is that in Lurefjorden, Western Norway (Fosså, 1992; Eiane *et al.*, 1999; Jarms *et al.*, 1999; Youngbluth and Båmstedt, 2001; Sørnes *et al.*, 2007). This occurrence probably appeared during the 1970s when fishermen first

doi:10.1093/plankt/fbq015, available online at www.plankt.oxfordjournals.org. Advance Access publication February 19, 2010

© The Author 2010. Published by Oxford University Press.

This is an Open Access article distributed under the terms of the Creative Commons Attribution Non-Commercial License (<http://creativecommons.org/licenses/by-nc/2.5/uk/>) which permits unrestricted non-commercial use, distribution, and reproduction in any medium, provided the original work is properly cited.

reported that their nets were clogged by *P. periphylla* (Fosså, 1992). Presently, three Norwegian mass occurrences have been reported in the scientific literature (Sørnes *et al.*, 2007), but several others have been observed, but not yet reported (J.-A. Sneli, personal communication; C. Schander, personal communication; K. Eiane, personal communication). Sørnes *et al.* (Sørnes *et al.*, 2007) investigated *P. periphylla* mass occurrences in three fjords: Lurefjorden, Halsafjorden and Sognefjorden. The main difference reported for these fjords was that Sognefjorden was dominated by small individuals (coronal diameter <4 cm) while the other fjords contained large numbers of all sizes. Sørnes *et al.* (Sørnes *et al.*, 2007) hypothesized that both the large and the small individuals were retained in Lurefjorden and Halsafjorden. First, the high light attenuation provided a suitable dark habitat in these fjords, and secondly shallow advective layers ensured little advective loss of individuals from these two fjords. Sørnes *et al.* (Sørnes *et al.*, 2007) termed this phenomenon, optically conditioned retention (termed “optical retention” below), due to the effect from the water column light attenuation. In contrast to Lurefjorden and Halsafjorden, Sørnes *et al.* (Sørnes *et al.*, 2007) hypothesized that the large individuals of Sognefjorden were exposed to a relatively deep advective layer that caused a high advective loss and little retention for this size group. The small individuals, however, were retained inside the fjord because they presumably require a dark habitat which was situated much deeper than the advective layer. While the mass occurrence in Sognefjorden was described as far back as in 1913 (Broch, 1913), the other two appear to have been established more recently (Sørnes *et al.*, 2007). Lately, it has been speculated that the light attenuation of the Norwegian Coastal Water, which affects the water masses of the fjords (Sætre, 2007), has increased over time (Eiane *et al.*, 1999; Sørnes *et al.*, 2007). Evidence for such long-term coastal water darkening has recently been provided (Aksnes *et al.*, 2009).

Here we have investigated the hypothesis (Sørnes *et al.*, 2007) that optically conditioned retention might facilitate mass occurrences of *Periphylla periphylla*. We apply a previously tested individual-based model of light-dependent swimming behaviour to simulate how the retention of *P. periphylla* is affected by light attenuation and topographic characteristics. Finally, we apply the model for different sets of topographic values that represent six fjords at the western coast of Norway.

METHOD

A model of light sensitivity of *P. periphylla*

We used a previously reported individual-based model that is described in detail in Dupont *et al.* (Dupont *et al.*,

2009), and where the main assumptions are briefly explained below. It is assumed that the vertical distance swum by an individual medusa, ΔZ_{med} , during the time step, Δt (Table I), is:

$$\Delta Z_{\text{med}} = \alpha V \Delta t \tag{1}$$

where α is a behavioural variable that takes either the value 1 (movement towards higher light) or -1 (movement towards less light), and V is the vertical swimming speed chosen randomly from a distribution based on acoustical observations reported in Dupont *et al.* (Dupont *et al.*, 2009).

Since the light intensity decreases with depth, $\alpha = 1$ corresponds to movement towards the surface and $\alpha = -1$ towards the bottom. These boundaries constrain the movement so that if equation (1) suggests a new location “below the bottom depth” after the time step Δt , the bottom acts as a mirror. The surface boundary is represented in the same way.

The ambient light (E_{med}) at the depth (Z_{med}) of an individual determines which value α takes at each time step (see what follows). E_{med} is calculated according to the Beer–Lambert law, $E_{\text{med}} = E_0 \exp(-K Z_{\text{med}})$, E_0 is the surface irradiance and K is the attenuation for downwelling irradiance between the surface and the depth E_{med} . We used the mechanism that gave the best fit with observations in Dupont *et al.* (Dupont *et al.*, 2009) to set the α value for each individual at each time step (Fig. 1). If the value of E_{med} is between E_{min} and

Table I: Parameter values used in the individual based simulation model

Parameter	Value	Unit	
Surface irradiance at night	1.23×10^{-7}	dim.	
Δt	21.55	s	
T_{sim}	315.36×10^5	s	
t_{lethal}	2229.12×10^3	s	
N	320	Individual	
	Large	Small	
	<i>P. periphylla</i>	<i>P. periphylla</i>	
$\overline{E_{\text{max}}}$	7.38×10^{-6}	1.37×10^{-8}	dim.
$\overline{E_{\text{min}}}$	1.1×10^{-9}	2.97×10^{-10}	dim.
$\sigma_{\overline{E_{\text{max}}}}^2$	2.55×10^{-10}	9.49×10^{-16}	dim.
$\sigma_{\overline{E_{\text{min}}}}^2$	5.71×10^{-18}	4.45×10^{-19}	dim.

The light thresholds $\overline{E_{\text{min}}}$ and $\overline{E_{\text{max}}}$ correspond to the calculated relative light intensity at the two depths $Z_m + Z_s$ and $Z_m - Z_s$ that is reported in Table 4 in Sørnes *et al.* (2007). These depths represent the mean depth ± 1 standard deviation of the vertical *P. periphylla* distributions that were observed in Lurefjorden and Sognefjorden. The corresponding $\sigma_{\overline{E_{\text{max}}}}^2$ and $\sigma_{\overline{E_{\text{min}}}}^2$ for both size classes are calculated according to Dupont *et al.* (2009): $\sigma_{\overline{E_{\text{min}}}}^2 = (2.25 \overline{E_{\text{min}}})^2$ and $\sigma_{\overline{E_{\text{max}}}}^2 = (2.17 \overline{E_{\text{max}}})^2$. The value of t_{lethal} was approximated from Jarms *et al.* (2002) as the mean of the observed survival time under light exposure. Δt , T_{sim} , N are the time step, the duration of and the number of individuals assumed in each simulation. Dimensionless quantities are indicated by dim.

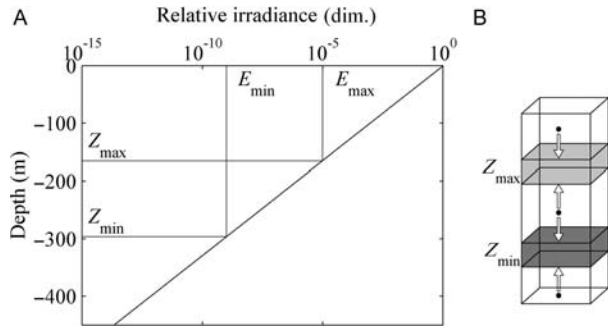


Fig. 1. Conceptual scheme of the swimming model modified after Dupont *et al.* (Dupont *et al.*, 2009). **(A)** How z_{\max} and z_{\min} (in m) are related to E_{\max} and E_{\min} (dimensionless). **(B)** The arrows represent the possible swimming directions depending on the location of the individual in the water column (upward corresponds to $\alpha = 1$ and downward to $\alpha = -1$, see text). The shaded areas represent individual variations in z_{\max} and z_{\min} as a result of individual variances in E_{\max} and E_{\min} .

E_{\max} (Fig. 1A), α is set randomly at either -1 or 1 . Otherwise if E_{med} is lower than E_{\min} (which means that z_{med} is deeper than z_{\min}) or higher than E_{\max} (z_{med} is shallower than z_{\max}), α is set to 1 and -1 , respectively (Fig. 1B). The individual values of the E_{\min} and E_{\max} parameters are distributed according to a gamma distribution with the mean values $\overline{E_{\min}}$ and $\overline{E_{\max}}$ and the variances $\sigma_{E_{\min}}^2$ and $\sigma_{E_{\max}}^2$.

The light-related values used in the present study are given in Table I. Small and large individuals are differentiated as in Sørnes *et al.* (Sørnes *et al.*, 2007). The values of $\overline{E_{\min}}$ and $\overline{E_{\max}}$ that were applied in Dupont *et al.* (Dupont *et al.*, 2009) were tuned according to limited acoustical observations of large individuals of *P. periphylla* in Lurefjorden and were not applicable to the present study. The comparison of the vertical distribution of small and large *P. periphylla* in three fjords in Sørnes *et al.* (Sørnes *et al.*, 2007) suggests that the small individuals on average occupy a larger optical depth interval, i.e. a darker part of the water column, than the large individuals (Table 4 in Sørnes *et al.*, 2007). We therefore assume that the small individuals have lower light preferences than large individuals (Table I), and the $\overline{E_{\min}}$ and $\overline{E_{\max}}$ values were approximated from (i) the observed vertical distributions of small and large individuals of *P. periphylla* in Lurefjorden and Sognefjorden in April 2003 that was reported in Table 4 of Sørnes *et al.* (Sørnes *et al.*, 2007), (ii) a relative surface light intensity for mid-April compared with the sunniest Julian day ($\overline{E_{\min}}$ and $\overline{E_{\max}}$ are then relative dimensionless light intensity values) and (iii) the light attenuations derived for these two fjords in Aksnes *et al.* (Aksnes *et al.*, 2009) in 2006 (Table II). Thus, we have applied non-simultaneous measurements of *P. periphylla* distribution and light attenuation in defining the values

of $\overline{E_{\min}}$ and $\overline{E_{\max}}$. Although the difference in light attenuation between the two fjords appears to be relatively persistent over years (Sørnes and Aksnes, 2006), even slight changes from 2003 to 2006 are likely to have introduced order-of-magnitude errors in the $\overline{E_{\min}}$ and $\overline{E_{\max}}$ estimates we have applied. This is due to the exponential nature of the attenuation of light with depth and that the E -estimates we apply reflect the light intensities at greater depths in the range 101–1210 m (Sørnes *et al.*, 2007). The consequences of inaccuracies in this approximation are investigated in an analysis where the sensitivity of retention is investigated as a function of variation in $\overline{E_{\min}}$ and $\overline{E_{\max}}$.

Simulated light intensity

The astronomical equation of Brock (Brock, 1981) was used to calculate the energy received at the top of the atmosphere as a function of time of year and latitude:

$$E_{\text{ta}} = \frac{E_{\text{sc}} \cos(\zeta)}{R^2} \quad (2)$$

where E_{ta} is the top atmosphere irradiance, E_{sc} is the solar constant, ζ is the zenith angle and R the radius vector expressing the distance from the earth to the sun taking in account the elliptic orbit of the earth. R is calculated depending on the Julian day. The cosine of ζ is calculated from other astronomical parameters according to Brock (Brock, 1981).

This value was then corrected for atmospheric attenuation (Smith and Dobson, 1984) to provide the sea surface irradiance, E_0 ,

$$E_0 = E_{\text{ta}} \left[\text{Rad} + \text{El}^{D_0/\text{El}} \right]. \quad (3)$$

Here we have ignored the effect of variations in cloud cover by assuming a clear sky. Rad is the diffuse radiation, El the solar elevation and D_0 the optical density of the atmosphere.

Similar to the values of $\overline{E_{\min}}$ and $\overline{E_{\max}}$, we transformed E_0 into a relative value of surface irradiance (dimensionless):

$$E_{\text{rel0}} = \frac{E_0}{E_{\text{june}}} \quad (4)$$

where E_{june} is the light surface irradiance the sunniest day of the year i.e. the 21st of June.

As in Dupont *et al.* (Dupont *et al.*, 2009), we assumed a constant night light irradiance of $4.6 \times 10^{-4} \mu\text{mol photons m}^{-2} \text{s}^{-1}$ which corresponds to the relative value of 1.23×10^{-7} .

Table II: Vertical profiles of the light attenuation coefficient at 500 nm (K_{500} , m^{-1}) for the six simulated fjords

Depth	Lurefjorden	Masfjorden	Lysefjorden	Sognefjorden	Sandsfjorden	Jøsenfjorden
2	–	–	0.323	–	–	–
5	–	–	0.233	0.120	0.253	0.119
10	0.227	0.122	0.162	0.100	0.075	0.110
15	–	–	–	0.092	–	–
20	0.172	0.102	0.126	0.083	0.059	0.088
25	–	–	–	0.069	–	–
30	–	–	–	0.057	–	–
40	0.107	0.088	0.058	0.041	0.046	0.094
50	–	–	–	0.047	–	–
60	–	0.069	0.065	0.043	0.064	0.077
100	0.088	0.050	0.098	0.038	0.066	0.058
150	0.100	0.066	0.067	0.023	–	–
200	0.110	0.047	0.061	0.025	0.059	0.046
250	0.120	0.039	0.040	0.031	–	–
300	0.137	0.058	0.066	0.029	0.069	0.072
400	0.117	0.073	0.112	0.026	0.129	0.099
450	–	0.085	–	–	0.111	–
500	–	–	–	0.025	–	0.107
600	–	–	–	0.039	–	0.118
800	–	–	–	0.047	–	–
1000	–	–	–	0.045	–	–
1200	–	–	–	0.054	–	–

The values were based on modified measurements of light absorption ($a_m(500)$) that were converted according to the relationship $K_{500} = 1.059a_m(500) + 0.013$ (Aksnes *et al.*, 2009).

Advection and passive drift of *P. periphylla*

It is assumed that individuals located in the advective layer of a fjord, defined as the layer between the surface and the sill depth, are passively drifting in or out of the fjord according to the horizontal currents that characterize this layer (Aksnes *et al.*, 1989; Sørnes *et al.*, 2007). This exchange of the advective layer was characterized by the fraction of the advective layer that is renewed per time unit, F_{fjord} (s^{-1}) (Salvanes *et al.*, 1995):

$$F_{\text{fjord}} = \frac{S_{\text{adv}} A_{\text{sill}}}{V_{\text{adv}}} \quad (5)$$

where S_{adv} ($m s^{-1}$) represents the mean current in the advective layer, A_{sill} is the cross-sectional area (m^2) above the sill depth and V_{adv} is the volume of the advective layer of the fjord (m^3). If an individual occupies the advective layer for a period, Δt , we assume that the probability that this individual is not lost from the fjord (i.e. retained) in this period corresponds to $\exp(-F_{\text{fjord}}\Delta t)$, and a lower exposure time in the advective layer will cause a higher retention. An individual that always occupies the basin water (i.e. below sill depth) will not be lost through advection in our simulations and will have maximal retention. During a simulation, we calculated the total time P_i (s) each individual was located in the advective layer:

$$P_i = x_i \Delta t \quad (6)$$

where x_i is the number of time steps (Δt , s) spent in the advective layer for individual i during the entire simulated period T_{sim} (Table I). The individual advective loss rate (s^{-1}) is then:

$$F_i = \frac{F_{\text{fjord}} P_i}{T_{\text{sim}}} \quad (7)$$

The chance that an individual is retained in the fjord during a simulation is then $\text{ret}_i = \exp(-F_{\text{fjord}} P_i)$ and the retention i.e. non-advection of the simulated population (\mathcal{N}) is:

$$\text{ret} = \sum_{i=1}^{\mathcal{N}} \frac{\text{ret}_i}{\mathcal{N}} \quad (8)$$

A ret equals to one means that all individuals are retained in the fjord during the simulation. In that case, the advective loss, which is defined as $\text{adv} = 1 - \text{ret}$, becomes zero. So far we have assumed no mortality, but in the next paragraph this is introduced.

Mortality

According to Jarms *et al.* (Jarms *et al.*, 2002), light exposure turns the natural pigment of *P. periphylla* into a toxic substance lethal to the individuals. In locations where the bottom depth is too shallow to provide the sufficient darkness at daytime, the vertical migration model (Dupont *et al.*, 2009) forces the simulated

Table III: Assumed topographical characteristics for the six fjords

	Lurefjorden	Masfjorden	Lysefjorden	Sognefjorden	Sandsfjorden	Jøsenfjorden	Unit
Bottom depth	439	494	460	1304	510	640	m
Sill depth	20	75	14	165	110	90	m
Sill area (A_{sill})	3000	108000	12 900	88 100	157 300	603 000	m ²
Volume of advective layer (V_{adv})	0.78×10^9	1.97×10^9	0.66×10^9	157×10^9	9.31×10^9	3.67×10^9	m ³
Current (S_{adv})	0.08	0.08	0.08	0.08	0.08	0.08	m s ⁻¹
F_{fjord}	3.08×10^{-7}	43.86×10^{-7}	15.63×10^{-7}	0.45×10^{-7}	13.52×10^{-7}	131.44×10^{-7}	s ⁻¹

Lurefjorden, Masfjorden, Sognefjorden (Sørnes and Aksnes, 2006), Sandsfjorden, Jøsenfjorden (Kaartvedt and Svendsen, 1995) and Lysefjorden (Aure et al., 2007). Topographical characteristics that were not explicitly given as numbers in the sited studies were extracted from figures by using Adobe® Acrobat® Professional. The average current rate of the advective layer was taken from Aksnes et al. (1989) in their study of Masfjorden.

individual to “bump” against the bottom in a too illuminated environment. If the time period an individual is exposed to this situation exceeds t_{ethal} (Table I), death is invoked for this individual. The fraction (S) of the initial population (N) that survives a simulation is then:

$$S = \frac{N_{\text{surv}}}{N} \tag{9}$$

where N_{surv} is the number of individual that has been tagged alive at the end of a simulation. While ret in equation (8) is the retention in the case where there is no mortality (i.e. $S = 1$), we define the optical retention:

$$R = \sum_{i=1}^{N_{\text{surv}}} \frac{ret_i}{N} \tag{10a}$$

which means that the optical retention is affected by the light-induced mortality loss as well as the advective loss as hypothesized by Sørnes et al. (Sørnes et al., 2007). How these two losses affect R is explicitly seen if we combine equation (10a) with equation (9) and define $ret_{\text{surv}} = \sum_{i=1}^{N_{\text{surv}}} ret_i / N_{\text{surv}}$:

$$R = ret_{\text{surv}} S = (1 - adv_{\text{surv}})(1 - M) \tag{10b}$$

where the advective and the mortality losses are $adv_{\text{surv}} = 1 - ret_{\text{surv}}$ and $M = 1 - S$, respectively.

Sensitivity analysis

In a sensitivity analysis, we investigated how variations in the topographical characteristics and in the light attenuation affected the optical retention of *P. periphylla*. The light attenuation coefficient (K_{500} for the wavelength 500 nm) was varied over the range 0.02–0.14 m⁻¹. In order to simplify the interpretations of the analysis, we assumed four idealized fjords characterized by two discrete sill depths (10 and 100 m, which correspond to the thickness of the advective layers) and two discrete bottom depths (100 and 500 m), but later on we will consider continuous sill

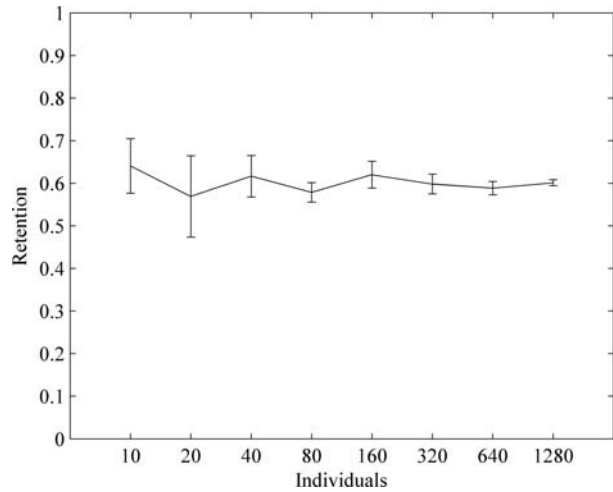


Fig. 2. Simulated retention in Lurefjorden (dimensionless) depending on the number of individuals used in the simulations. Confidence intervals (95%) for the mean optical retention ($n = 7$) are shown.

and bottom depths. In the sensitivity analysis, the exchange rate of the advective layer, F_{fjord} , was kept constant at $3.08 \times 10^{-7} \text{ s}^{-1}$ which corresponds to that approximated for Lurefjorden (Table III). We used 320 individuals in the simulations. This number ensured relatively low computation time and acceptable uncertainty (Fig. 2).

Simulation of optical retention in six fjords

The optical retention was simulated for different sets of topographic values representing six existing fjords (Fig. 3): Sognefjorden (61°08.3'N 6°08.8'E), Masfjorden (60°49.6'N 5°20.7'E), Lurefjorden (60°41.7'N, 5°08.5'E), Sandsfjorden (59°30.2'N, 6°19.5'E), Jøsenfjorden (59°17.2'N, 6°18.7'E) and Lysefjorden (59°00.5'N, 6°20.2'E). Topographical characteristics are given in Table III. The light attenuations of the six fjords (Table II) were based on measurements during a cruise in November 2006 (Aksnes et al., 2009). In a second sensitivity analysis, we studied how variations in the estimated light preference of *P. periphylla* (i.e. $\overline{E_{\text{min}}}$ and $\overline{E_{\text{max}}}$) affect the simulated retention of *P. periphylla* within a fjord.

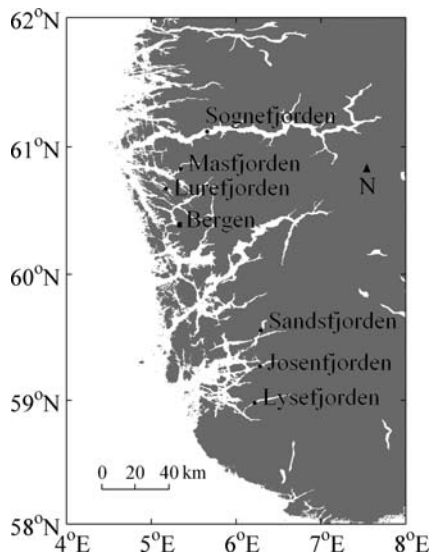


Fig. 3. Location of the six simulated fjords in southwest Norway. Topographical characteristics are given in Table III.

RESULTS

Sensitivity analysis

Survival

Large individuals (Fig. 4A) have a higher survival at low light attenuation than the small ones (Fig. 4B). This is because the large individuals are assumed to tolerate higher light intensity than the small individuals (i.e. higher \bar{E}_{\max} value for the large individuals, see Table I). For both size classes, the deep fjord (500 m) provides a higher survival than the shallow fjord simply because this fjord provides a larger vertical habitat that satisfies the assumed light preferences of *P. periphylla* (Fig. 4A and B). In the shallow fjord, the large individuals have a survival close to 1 for attenuations above 0.08 m^{-1} , indicating that individuals survive throughout the simulated period (1 year). Increased attenuation shoals and narrows the vertical habitat of large *P. periphylla* and lethal light exposure at the bottom is therefore avoided. This is not the case for the small individuals in the shallow fjord where lethal light exposure results in a survival close to 0 also at the highest attenuation. It can be concluded that an increase in both the bottom depth and the light attenuation has the same positive effect on survival through facilitation of a darker habitat.

Advective loss

The increased light attenuation leads to increased advective loss, i.e. more individuals are transported out of the fjord (Fig. 5A and B). This is clearly seen for the deep sill (100 m) combined with high attenuation which

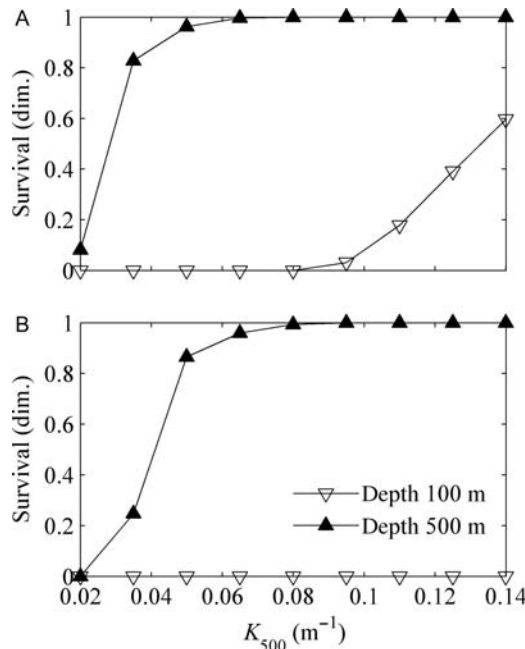


Fig. 4. Survival [S dimensionless as defined in equation (9)] as a function of light attenuation (K_{500}, m^{-1}) for a shallow (100 m) and a deep (500 m) fjord. (A) Large individuals, (B) small individuals. The sill depth of the fjords was set equal to 10 m.

leads to an advective loss above 0.9 for both size groups (Fig. 5A and B). The explanation is that the high light attenuation has shoaled the habitat of *P. periphylla* so it becomes part of the advective layer. The small individuals always have the lowest advective loss since their preference for lower light (Table I) results in a deeper location than that of the larger individuals. Also for the shallow sill (10 m), the advective loss increases with increased attenuation (Fig. 5A and B) although less than for the deep sill fjord. Thus, while increased attenuation increases survival, it also increases the advective loss which imposes opposite effects on the retention as defined in equation (10).

Optical retention

We have shown above that an increased light attenuation diminishes the lethal light exposure of individuals but at the same time increases the exposure to the advective layer, which means that increased light attenuation does not necessitate increased retention. In terms of retention, a general pattern emerges where the maximal retention is obtained for an “optimal” light attenuation, and where retention decreases at both sides of this light attenuation optimum. This pattern is clearly demonstrated in the case of a deep fjord with a deep sill (Fig. 6A) where the optimal attenuations are in the range $0.03\text{--}0.05 \text{ m}^{-1}$, but also in the case of a deep

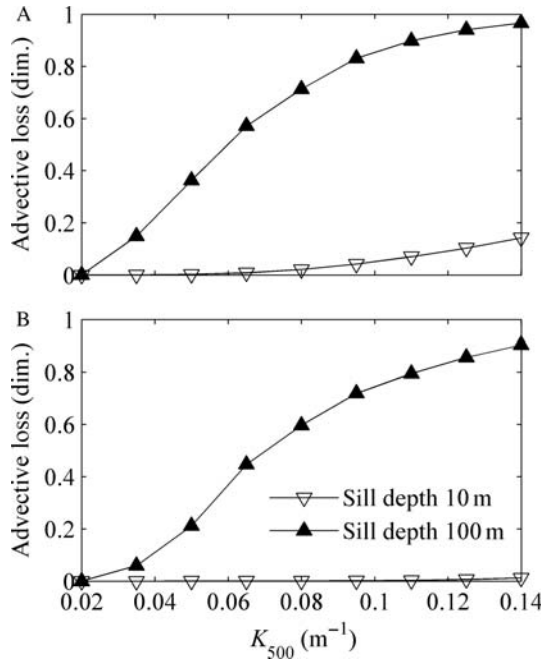


Fig. 5. Advective loss [adv_{surv} dimensionless as defined in equation (10b)] as a function of light attenuation (K_{500} , m^{-1}) for two fjords with a shallow (10 m) and a deep (100 m) sill. (A) Large individuals, (B) small individuals. The bottom depth of the fjords was set equal to 500 m.

fjord with a shallow sill (Fig. 6B). The case in Fig. 6B provides the highest retention which is caused by little advective loss of individuals (because of a shallow sill), but also by the increased survival seen at light attenuations above $0.05 m^{-1}$. Such attenuations ensure a sufficient dark habitat all the way down to the bottom. The last case (Fig. 6C), represented by a shallow fjord with a shallow sill, does not reveal light attenuation optima as these are situated outside the graph (i.e. at light attenuations higher than $0.14 m^{-1}$, Fig. 6C).

The assumed difference in the light preferences of small and large individuals (Table I) results in different attenuation optima for the two size groups. Thus, another general result that emerges from this sensitivity analysis is that a change in the light attenuation of a particular fjord might cause unequal opportunities for the retention of small and large *P. periphylla* as well as for other organisms with a light preference.

Simulation of optical retention in six fjords

Sandsfjorden and Jøsefjorden have the lowest simulated retention with values below 0.23 and 0.40 for large and small individuals, respectively. Thereafter follow Masfjorden, Sognefjorden and Lurefjorden, while Lysefjorden has the highest optical retention with

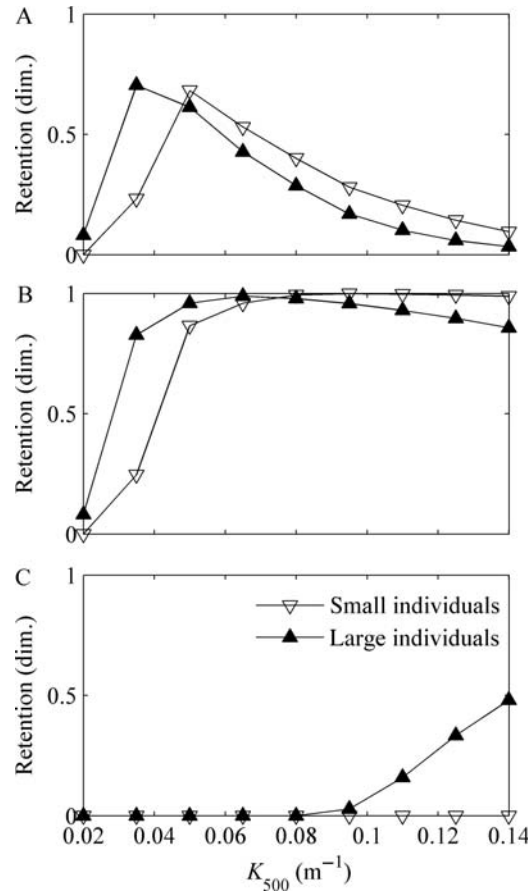


Fig. 6. Retention [R dimensionless as defined in equation (10)] as a function of light attenuation (K_{500} , m^{-1}) for large and small individuals. (A) A deep (500 m) fjord with a deep sill (100 m). (B) A deep (500 m) fjord with a shallow sill (10 m). (C) A shallow fjord (100 m) with a shallow sill (10 m).

values of 0.71 and 0.92 for large and small individuals, respectively. For all fjords, the large individuals have a lower optical retention than the small individuals because we have assumed higher light preferences for the large individuals. When the values of the light attenuation, K_{500} , are increased by 25% (i.e. darker water than the values indicated in Table II), the optical retention decreases for both size groups for all fjords. This simulation result clearly opposes the suggestion that increased light attenuation increases the likelihood for mass occurrences (Sørnes *et al.*, 2007), but the validity of this result critically depend on the assumed light preference values of *P. periphylla* (Table I). When these values are changed, so does the simulated optical retention. In Table I, it was assumed that $\overline{E_{max}} = 7.38 \times 10^{-6}$ for the large individuals. This gives a simulated retention of 0.32 for e.g. Masfjorden (Fig. 7). If $\overline{E_{max}}$ is altered as well as $\overline{E_{min}}$ (Fig. 7), however, a maximal retention of 0.97 is obtained for $\overline{E_{max}}$ close to 10^{-10} .

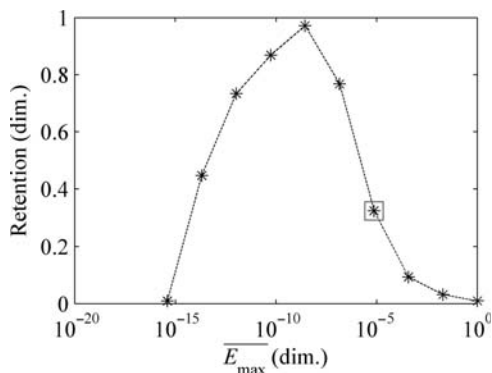


Fig. 7. Sensitivity of the simulated retention [R dimensionless as defined in equation (10)] to the values of the light preference parameters (\bar{E}_{\max} and \bar{E}_{\min}) of *P. periphylla*. Only the value of \bar{E}_{\max} are indicated on the x -axis, but the value of \bar{E}_{\min} was also varied so that it was about four orders of magnitude lower than \bar{E}_{\max} . The box indicates the light preference value assumed in Table I. The topography and light regime of Masfjorden was assumed in the sensitivity analysis.

This demonstrates that accurate simulations require accurate estimates of the light preference parameters, but also of the water column light attenuation. As emphasized in Method and further discussed below this has implications for the interpretation of the simulation results for the six fjords (Table IV).

DISCUSSION

For organisms where horizontal transportation is dominated by advection, as in plankton, vertical rather than horizontal behaviour is important for geographical retention of a population. Sørnes *et al.* (Sørnes *et al.*, 2007) suggested that such retention for *P. periphylla* was optically conditioned, and further hypothesized that increased attenuation of the Norwegian Coastal Water has increased the likelihood for retention and consequently mass occurrences in some Norwegian fjords. Given the assumption that the vertical behaviour of

P. periphylla is light sensitive (Dupont *et al.*, 2009), our present study demonstrates how the retention of *P. periphylla* is affected by different combinations of sill depth, basin depth and light attenuation. Increased light attenuation increases the simulated retention of *P. periphylla* through increased survival in fjords that otherwise would be too illuminated. However, our results also suggest that increased light attenuation might decrease the retention through increased exposure to the advective layer. This antagonistic effect of light attenuation on retention suggests that fjords can be classified into three categories. Category 1 corresponds to fjords with low attenuation (i.e. clear water) where the habitat of *P. periphylla* is constrained by high irradiance levels all the way down to the bottom. This category corresponds to that part of the curves in Fig. 6 where the optical retention increases with increased attenuation. Category 2 corresponds to fjords where the retention is maximal, i.e. where the light attenuation is optimal. Here, increased as well as decreased light attenuation will decrease the retention. Finally, category 3 corresponds to fjords where the light attenuation is superior to the optimal attenuation and retention decreases with increased light attenuation. This is caused by loss of individuals due to the increased advective exposure. This general classification should apply all planktonic organisms that have a light preference and the ability to adjust their depth accordingly.

As discussed in Aksnes *et al.* (Aksnes *et al.*, 2004), it is convenient to summarize the light environment of a fjord (or more generally for a water column) by the optical bottom depth (OD):

$$OD = K_{500} \zeta \tag{11}$$

where ζ (m) is the bottom depth of the fjord and K_{500} (m^{-1}) is the light attenuation of the water column. The optical bottom depth can be interpreted as an index of the darkness of a fjord, i.e. increasing OD means a darker fjord regardless of the cause (i.e. increased light

Table IV: Simulated retention for the six fjords

Fjord	Jøsenfjorden	Sandsfjorden	Masfjorden	Sognefjorden	Lurefjorden	Lysefjorden
Large individuals						
$K_{500} - 25\%$	0.48 (+128%)	0.46 (+109%)	0.56 (+75%)	0.67 (+62%)	0.79 (+36%)	0.88 (+24%)
K_{500}	0.21	0.22	0.32	0.42	0.58	0.71
$K_{500} + 25\%$	0.09 (−56%)	0.10 (−55%)	0.16 (−40%)	0.24 (−43%)	0.41 (−30%)	0.53 (−25%)
Small individuals						
$K_{500} - 25\%$	0.65 (+67%)	0.59 (+59%)	0.67 (+40%)	0.81 (+47%)	0.95 (+20%)	0.93 (+1%)
K_{500}	0.39	0.37	0.48	0.56	0.79	0.92
$K_{500} + 25\%$	0.24 (−39%)	0.23 (−38%)	0.32 (−33%)	0.37 (−32%)	0.58 (−26%)	0.77 (−16%)

Retention is shown for large (>4 cm) and small (<4 cm) individuals. The light attenuation K_{500} was decreased and increased by 25%, relative to the values in Table II. The result of these changes on the retention is shown in brackets as a percentage change.

attenuation and/or bottom depth). Our model predicts that the optical retention of *P. periphylla* is affected by the bottom depth as well as the light attenuation. These two variables, however, are combined in the dimensionless optical bottom depth. If we also represent the sill depth (i.e. the thickness of the advective layer) as a fraction of the bottom depth, our simulation results can be presented more generally. In contrast to the discrete sill chosen in the sensitivity analysis (Figs 5 and 6), it is now continuous. Figure 8 illustrates the variations in retention when the sill depth is a continuous variable. We see that the highest retention is obtained with a shallow relative sill depth and a high optical bottom depth for both small and large individuals (Fig. 8). The three fjord categories discussed earlier are indicated as shaded areas in Fig. 8. It can be seen that if the two dimensionless characteristics of a fjord fit into category 1 (light grey area in Fig. 8), an increase in the light attenuation (or in the bottom depth) of that fjord will increase the optical bottom depth and move the fjord closer to category 2 (grey area) which provides a higher optical retention of *P. periphylla*. On the other hand, if a fjord is of category 3 a decrease in the light attenuation (or in the bottom depth) is required to promote higher optical retention.

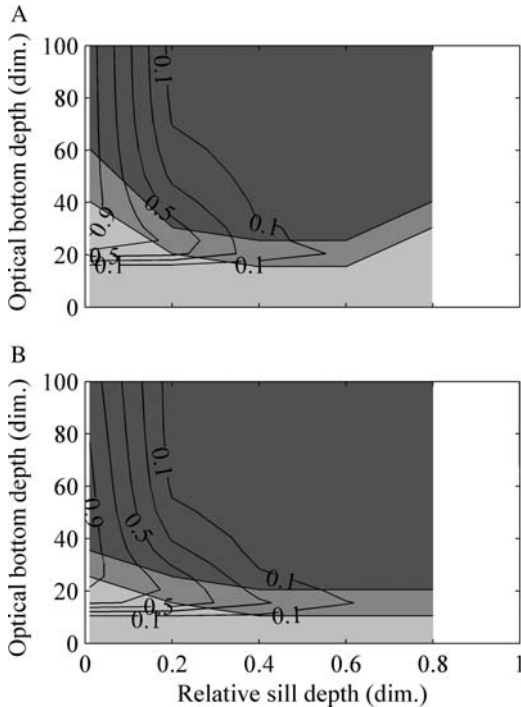


Fig. 8. Isolines of retention [R as defined in equation (10)] as a function of the optical bottom depth and the ratio between the sill and the bottom depth. Both axes are dimensionless (dim.). (A) Small and (B) large individuals. The light grey, grey and dark areas represent categories 1, 2, and 3 (see text), respectively.

It should be noted that although it appears as if the depth is eliminated by use of two non-dimensional quantities, absolute depth is still assumed in the migration model [equation (1)] that underlies the results in Fig. 8. A bottom depth of 500 m was assumed in the simulation, but very similar results are obtained for depths > 100 m (data not shown).

The effect of changes in light attenuation in the six simulated fjords

Sørnes *et al.* (Sørnes *et al.*, 2007) hypothesized that retention and mass occurrences of *P. periphylla* have been stimulated by increased light attenuation of the Norwegian Coastal Water. Our sensitivity analysis suggests that this hypothesis is valid for locations of category 1, but not for locations of category 2 and 3. The simulations of the six fjords suggest that all these fjords belong to category 3. Contrary to the hypothesis of Sørnes *et al.* (Sørnes *et al.*, 2007), this provides the prediction that increased attenuation tends to decrease the retention of *P. periphylla* (Table IV). However, as demonstrated in Fig. 7, which category a particular fjord fall into is in addition to light attenuation and sill depth sensitive to the parameterization of the light-mediated behaviour of *P. periphylla* (i.e. the values of \overline{E}_{\max} , \overline{E}_{\min} , and t_{ethal} in Table I). Because these parameterizations are based on rough approximations (see Method), our results on which category the fjords actually belong cannot be considered conclusive. Setting $\overline{E}_{\max} = 10^{-10}$, rather than 10^{-5} , all fjords are moved from category 3 into category 1 or 2 as illustrated with Masfjorden (Fig. 7). Consequently, predictions on how light attenuation affects retention in real fjords are altered. Although the two \overline{E}_{\max} values differ by five orders of magnitude, this corresponds to a difference in light intensities found at depths only 100 m apart (at 200 and 300 m, respectively) if the light attenuation of Lurefjorden is assumed (Table II). This underlines the need for accurate determinations of the values of \overline{E}_{\max} , \overline{E}_{\min} , t_{ethal} as well as the water column light attenuation in order to accurately predict the effect of a changing light regime on *P. periphylla* retention and the likelihood for mass occurrences.

Simulated optical retention and *P. periphylla* mass occurrences

Out of the six fjords studied, mass occurrences of *P. periphylla* have been reported only for Lurefjorden and Sognefjorden (Broch, 1913; Fosså, 1992; Sørnes *et al.*, 2007). Concerning the *P. periphylla* abundances of the four other fjords, we have no quantitative observations.

Several research cruises have been conducted in these fjords the last 20 years and, although *P. periphylla* has not been specifically targeted, it is likely that any exceptional abundances of this species would have been noticed. Nevertheless, lack of relevant observations precludes a quantitative test of the simulations, but some qualitative comments can be made. The simulation results in Table IV suggest a relatively high retention factor (>0.5) for small individuals in Sognefjorden and for both small and large individuals in Lurefjorden which is consistent with the pattern observed in these two fjords (Sørnes *et al.*, 2007). However, the highest retention was simulated for Lysefjorden which to our knowledge does not have high occurrence of *P. periphylla*. This might suggest that Lysefjorden is a potential location for mass occurrence although our results need to be interpreted with care. First, as discussed earlier, the simulation results are affected by large uncertainties in the values of the *P. periphylla* light sensitivity parameters (Fig. 7). Second, our simplified model considers advective and light-related factors only, and ignores all other aspects of *P. periphylla* requirements as well as characteristics of the population dynamics. For example, potential variation in the sources of mortality, such as predation, will obviously affect the likelihood for *P. periphylla* mass occurrences. In the dark fishless (Eiane *et al.*, 1999; Bagoien *et al.*, 2001), Lurefjorden *P. periphylla* seems to be long lived and have a low mortality rate (Jarms *et al.*, 1999). In the more fish rich fjords Masfjorden and Sognefjorden (Bagoien *et al.*, 2001) where waters are much clearer (Eiane *et al.*, 1999; Sørnes *et al.*, 2007), visual predation on *P. periphylla* might be higher (although we have no information about predation on *P. periphylla*). Competition with visual predators for zooplankton prey (Eiane *et al.*, 1999) in fish rich fjords may also affect the abundance of *P. periphylla* more than in e.g. Lurefjorden. Finally, reproduction processes are not well known in *P. periphylla*. The species has a complete development in the water column without a benthic phase (Jarms *et al.*, 1999), but little is known about the fecundity of the species. Thus, more knowledge on the biological and ecological aspects that have been ignored in our model is obviously needed to fully understand the *P. periphylla* mass occurrence phenomenon. Nevertheless, our results demonstrate that accurate knowledge of the deep water light regime as well as the light preferences of *P. periphylla* is likely to advance our understanding of its habitat requirements and the implications for mass occurrence. Models and analyses of environmental change often ignore the water column light regime except for photosynthesizing organisms. Although *P. periphylla* is considered to be a tactile non-visual

forager (Sørnes *et al.*, 2007), the water column light regime appears to be an important feature of its habitat. Because light detection occurs in most organisms, the ecological implications of a changing light regime deserve more attention. This seems particularly true for the pelagic realm where the rapid vertical change in light intensity perhaps is the most prominent factor shaping heterogeneity in an otherwise homogenous habitat.

ACKNOWLEDGEMENTS

We would like to thank Andrew Yool for providing online the Matlab[®] (The MathWorks[™]) program code for light surface irradiance, as well as two anonymous reviewers for their input on earlier versions of the manuscript.

FUNDING

Financial support from the European Union Marie Curie Early Stage Training project METAOCEANS (MEST-CT-2005-019678) and the L. Meltzer Høyskolefond as well as two anonymous reviewers for their input on earlier versions of the manuscript.

REFERENCES

- Aksnes, D. L., Aure, J., Kaartvedt, S. *et al.* (1989) Significance of advection for the carrying capacities of fjord populations. *Mar. Ecol. Prog. Ser.*, **50**, 263–274.
- Aksnes, D. L., Nejtgaard, J., Sædberg, E. *et al.* (2004) Optical control of fish and zooplankton populations. *Limnol. Oceanogr.*, **49**, 233–238.
- Aksnes, D. L., Dupont, N., Staby, A. *et al.* (2009) Coastal water darkening and implications for mesopelagic regime shifts in Norwegian fjords. *Mar. Ecol. Prog. Ser.*, **387**, 39–49.
- Atrill, M. J., Wright, J. and Edwards, M. (2007) Climate-related increases in jellyfish frequency suggest a more gelatinous future for the North Sea. *Limnol. Oceanogr.*, **52**, 480–485.
- Aure, J., Strand, Ø., Erga, S. R. *et al.* (2007) Primary production enhancement by artificial upwelling in a western Norwegian fjord. *Mar. Ecol. Prog. Ser.*, **352**, 39–52.
- Bagoien, E., Kaartvedt, S., Aksnes, D. L. *et al.* (2001) Vertical migration and mortality of overwintering *Calanus*. *Limnol. Oceanogr.*, **46**, 1494–1510.
- Broch, H. (1913) Scyphomedusae from the “Michael Sars” North Atlantic deep-sea expedition 1910. “Michael Sars” *North Atlantic Deep-Sea Expedition 1910. Rep. Sci. Res.*, **3**, 1–23.
- Brock, T. D. (1981) Calculating solar radiation for ecological studies. *Ecol. Model.*, **14**, 1–19.
- Dupont, N., Klevjer, T. A., Kaartvedt, S. *et al.* (2009) Diel vertical migration of the deep water jellyfish *Periphylla periphylla* simulated as individual responses to absolute light intensity. *Limnol. Oceanogr.*, **54**, 1765–1775.

- Eiane, K., Aksnes, D. L., Bagoien, E. *et al.* (1999) Fish or jellies—a question of visibility? *Limnol. Oceanogr.*, **44**, 1352–1357.
- Fosså, J. H. (1992) Mass occurrence of *Periphylla periphylla* (Scyphozoa, Coronatae) in a Norwegian fjord. *Sarsia*, **77**, 237–251.
- Jarms, G., Bamstedt, U., Tiemann, H. *et al.* (1999) The holopelagic life cycle of the deep-sea medusa *Periphylla periphylla* (Scyphozoa, Coronatae). *Sarsia*, **84**, 55–65.
- Jarms, G., Tiemann, H. and Båmstedt, U. (2002) Development and biology of *Periphylla periphylla* (Scyphozoa: Coronatae) in a Norwegian fjord. *Mar. Biol.*, **141**, 647–657.
- Kaartvedt, S. and Svendsen, H. (1995) Effect of freshwater discharge, intrusions of coastal water, and bathymetry on zooplankton distribution in a Norwegian fjord system. *J. Plankton Res.*, **17**, 493–511.
- Lo, W.-T., Purcell, J. E., Hung, J.-J. *et al.* (2008) Enhancement of jellyfish (*Aurelia aurita*) populations by extensive aquaculture rafts in a coastal lagoon in Taiwan. *ICES J. Mar. Sci.*, **65**, 453–461.
- Lynam, C. P., Hay, S. J. and Brierley, A. S. (2004) Interannual variability in abundance of North Sea jellyfish and links to the North Atlantic Oscillation. *Limnol. Oceanogr.*, **49**, 637–643.
- Mills, C. E. (2001) Jellyfish blooms: are populations increasing globally in response to changing ocean conditions? *Hydrobiologia*, **451**, 55–68.
- Purcell, J. E. (2005) Climate effects on formation of jellyfish and ctenophore blooms: a review. *J. Mar. Biol. Assoc. UK*, **85**, 461–476.
- Purcell, J. E. and Arai, M. N. (2001) Interactions of pelagic cnidarians and ctenophores with fish: a review. *Hydrobiologia*, **451**, 27–44.
- Purcell, J. E., White, J. R., Nemazie, D. A. *et al.* (1999) Temperature, salinity and food effects on asexual reproduction and abundance of the scyphozoan *Chrysaora quinquecirrha*. *Mar. Ecol. Prog. Ser.*, **180**, 187–196.
- Purcell, J. E., Uye, S. and Wen-tseng, L. (2007) Anthropogenic causes of jellyfish blooms and their direct consequences for humans: a review. *Mar. Ecol. Prog. Ser.*, **350**, 153–174.
- Salvanes, A. G. V., Aksnes, D., Fosså, J. H. *et al.* (1995) Simulated carrying capacities of fish in Norwegian fjords. *Fish. Oceanogr.*, **4**, 17–32.
- Smith, S. D. and Dobson, F. W. (1984) The heat budget at ocean weather station Bravo. *Atmos. Ocean*, **22**, 1–22.
- Sørnes, T. A. and Aksnes, D. L. (2006) Concurrent temporal patterns in light absorbance and fish abundance. *Mar. Ecol. Prog. Ser.*, **325**, 181–186.
- Sørnes, T. A., Aksnes, D. L., Båmstedt, U. *et al.* (2007) Causes for mass occurrences of the jellyfish *Periphylla periphylla*: a hypothesis that involves optically conditioned retention. *J. Plankton Res.*, **29**, 157–167.
- Sætre, R. (2007) *The Norwegian Coastal Current*. Tapir Academic press, Trondheim.
- Youngbluth, M. J. and Båmstedt, U. (2001) Distribution, abundance, behavior and metabolism of *Periphylla periphylla*, a mesopelagic coronate medusa in a Norwegian fjord. *Hydrobiologia*, **451**, 321–333.